

See discussions, stats, and author profiles for this publication at: <https://www.researchgate.net/publication/233400199>

# Dynamics of magnetic nanoparticle in a viscous liquid: Application to magnetic nanoparticle hyperthermia

Article in Journal of Applied Physics · July 2012

DOI: 10.1063/1.4737126

CITATIONS

73

READS

655

3 authors, including:



Nikolai A. Usov

Russian Academy of Sciences

151 PUBLICATIONS 1,979 CITATIONS

[SEE PROFILE](#)



B. Ya. Liubimov

87 PUBLICATIONS 193 CITATIONS

[SEE PROFILE](#)

Some of the authors of this publication are also working on these related projects:



Project

Development of new types of magnetic nano heaters and promising micro-swimmers for the treatment of cancer and targeted drug delivery [View project](#)



Project

Properties of polycrystalline nanoparticles with uniaxial and cubic types of magnetic anisotropy of individual grains [View project](#)

## Dynamics of magnetic nanoparticle in a viscous liquid: Application to magnetic nanoparticle hyperthermia

N. A. Usov and B. Ya. Liubimov

Citation: *J. Appl. Phys.* **112**, 023901 (2012); doi: 10.1063/1.4737126

View online: <http://dx.doi.org/10.1063/1.4737126>

View Table of Contents: <http://jap.aip.org/resource/1/JAPIAU/v112/i2>

Published by the [American Institute of Physics](#).

---

### Related Articles

Low energy electron stimulated desorption from DNA films dosed with oxygen

*JCP: BioChem. Phys.* **6**, 06B614 (2012)

Low energy electron stimulated desorption from DNA films dosed with oxygen

*J. Chem. Phys.* **136**, 235104 (2012)

Induction of apoptosis in human breast cancer cells by a pulsed atmospheric pressure plasma jet

*Appl. Phys. Lett.* **97**, 023702 (2010)

Radiation damage in biomimetic dye molecules for solar cells

*J. Chem. Phys.* **131**, 214702 (2009)

Bounds and estimates for power absorption in two-dimensional highly lossy configurations

*J. Appl. Phys.* **95**, 8298 (2004)

---

### Additional information on J. Appl. Phys.

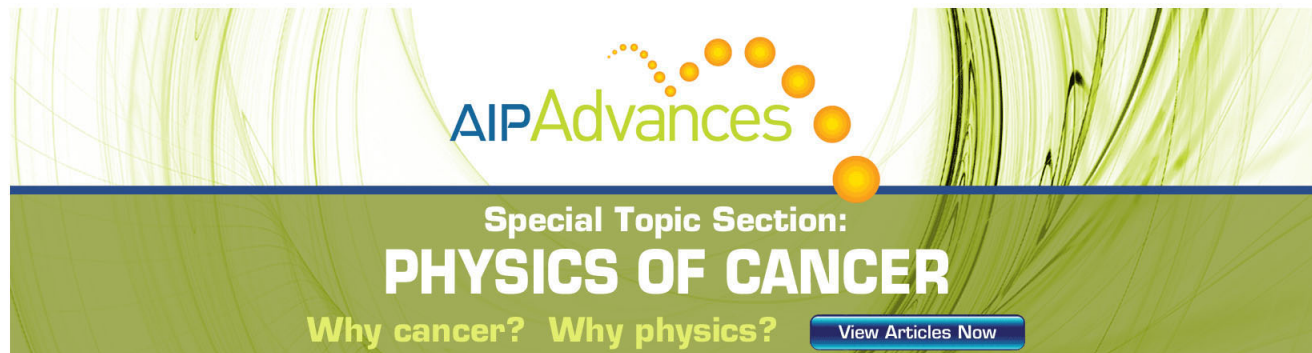
Journal Homepage: <http://jap.aip.org/>

Journal Information: [http://jap.aip.org/about/about\\_the\\_journal](http://jap.aip.org/about/about_the_journal)

Top downloads: [http://jap.aip.org/features/most\\_downloaded](http://jap.aip.org/features/most_downloaded)

Information for Authors: <http://jap.aip.org/authors>

## ADVERTISEMENT

The advertisement features a green and yellow abstract background with flowing lines. At the top, the 'AIP Advances' logo is displayed, with 'AIP' in blue and 'Advances' in green, accompanied by a series of orange dots. Below this, the text 'Special Topic Section: PHYSICS OF CANCER' is written in white, with 'PHYSICS OF CANCER' in a larger, bold font. At the bottom, the phrase 'Why cancer? Why physics?' is written in yellow, and a blue button with the text 'View Articles Now' is located on the right side.

**AIP Advances**

Special Topic Section:  
**PHYSICS OF CANCER**

Why cancer? Why physics? [View Articles Now](#)

# Dynamics of magnetic nanoparticle in a viscous liquid: Application to magnetic nanoparticle hyperthermia

N. A. Usov<sup>1,2</sup> and B. Ya. Liubimov<sup>1</sup>

<sup>1</sup>*Institute of Terrestrial Magnetism, Ionosphere and Radio Wave Propagation, Russian Academy of Sciences, (IZMIRAN), 142190 Troitsk, Moscow, Russia*

<sup>2</sup>*Magnetic and Cryoelectronic Systems Ltd., 142190 Troitsk, Moscow, Russia*

(Received 22 March 2012; accepted 10 June 2012; published online 18 July 2012)

It is shown that the magnetic dynamics of an assembly of nanoparticles dispersed in a viscous liquid differs significantly from the behavior of the same assembly of nanoparticles immobilized in a solid matrix. For an assembly of magnetic nanoparticles in a liquid two characteristic mode for stationary magnetization oscillations are found that can be called the viscous and magnetic modes, respectively. In the viscous mode, which occurs for small amplitude of the alternating magnetic field  $H_0$  as compared to the particle anisotropy field  $H_k$ , the particle rotates in the liquid as a whole. In a stationary motion the unit magnetization vector and the director, describing the spatial orientation of the particle, move in unison, but the phase of oscillations of these vectors is shifted relative to that of the alternating magnetic field. Therefore, for the viscous mode the energy absorption is mainly due to viscous losses associated with the particle rotation in the liquid. In the opposite regime,  $H_0 \geq H_k$ , the director oscillates only slightly near the external magnetic field direction, whereas the unit magnetization vector sharply jumps between magnetic potential wells. Thus, a complete orientation of the assembly of nanoparticles in the liquid occurs in the alternating magnetic field of sufficient amplitude. As a result, large specific absorption rates, of the order of 1 kW/g, can be obtained for an assembly of magnetic nanoparticles in viscous liquid in the transient,  $H_0 \sim 0.5H_k$ , and magnetic modes at moderate frequency and alternating magnetic field amplitude. © 2012 American Institute of Physics. [<http://dx.doi.org/10.1063/1.4737126>]

## I. INTRODUCTION

Superparamagnetic nanoparticles have actually found important applications in biomedicine, particularly for targeted drug delivery and magnetic nanoparticle hyperthermia.<sup>1,2</sup> To select an assembly of magnetic nanoparticles suitable in hyperthermia, it is important<sup>2-4</sup> to clarify the conditions that provide sufficiently high specific absorption rate (SAR) of the assembly in alternating external magnetic field of moderate amplitude  $H_0$  and frequency  $f$ . From a theoretical point of view, the behavior of an assembly of superparamagnetic nanoparticles in an alternating external magnetic field has been studied in detail<sup>5-9</sup> for the case when the uniaxial nanoparticles are immobilized in a surrounding solid matrix. In this case, only the particle magnetic moments can respond to the alternating external magnetic field, whereas the rotation of the particles as a whole is impossible. The description of the power absorption process<sup>5-9</sup> takes into account the thermal fluctuations of the particle magnetic moments at a finite temperature and uses the methods developed to study the Neel–Brown magnetization relaxation.<sup>10-12</sup> One of the most important results obtained for an assembly of immobilized nanoparticles is a significant SAR dependence on the magnetic parameters and average sizes of the nanoparticles, since these parameters determine the characteristic relaxation time  $\tau_N$  of the particle magnetic moment.

However, the most of the SAR measurements<sup>13-26</sup> were carried out for assemblies of magnetic nanoparticles dispersed in aqueous solutions or liquid mixtures of various vis-

cosities. In magnetic hyperthermia, the assembly of nanoparticles is likely to operate in a liquid medium, although in some cases the particles probably will be immobilized at the vessel walls or inside the biological cells.<sup>16</sup> It is therefore important to generalize the theoretical results<sup>5-9</sup> to the case of an assembly of nanoparticles in a viscous liquid. In a viscous medium, the particles can rotate as a whole both under the influence of the regular torque associated with the magnetic interactions and due to thermal fluctuations in the surrounding liquid. The process of the second type is usually described in the theory of Brownian relaxation<sup>27,28</sup> by introducing the corresponding relaxation time  $\tau_B$ .

The behavior of an assembly of magnetic nanoparticles in a viscous liquid is studied in details, in particular, in the theory of magnetic fluids.<sup>27-30</sup> In early papers by Newman and Yarbrough<sup>31,32</sup> the relaxation of the magnetic moment of an assembly of particles in a constant external magnetic field was considered neglecting the thermal fluctuations. Later, more general approach was developed to study magnetization relaxation<sup>33,34</sup> and complex magnetic susceptibility<sup>35-38</sup> of an assembly of magnetic nanoparticles in an alternating external magnetic field. It should be noted, however, that the low-frequency hysteresis loops of the assembly of nanoparticles in an alternating magnetic field of finite amplitude are still not investigated in detail. As a rule, the theoretical interpretation<sup>3,4,16,17,19,23,24</sup> of the behavior of an assembly of nanoparticles in a liquid in the alternating external magnetic field is based on the linear approximation.<sup>39</sup> Besides, it uses an assumption<sup>27,39</sup> that the magnetic

response of the assembly in a liquid can be characterized by the so-called effective relaxation time,  $\tau_{ef} = \tau_B \tau_N / (\tau_B + \tau_N)$ . Note that the linear approximation breaks down already in the moderate fields,  $H_0 = 200\text{--}300$  Oe, which are often used in the experiment. Besides, the concept of the effective relaxation time is not strictly justified.

Surely, both relaxation times,  $\tau_B$  and  $\tau_N$ , are essential to describe various aspects of the magnetic nanoparticle behavior in a liquid. However, the introduction of the effective relaxation time  $\tau_{ef}$  often oversimplifies the physical situation, since it does not take into account the complex dynamics of a magnetic nanoparticle in liquid. An attempt to overcome this difficulty was made in Ref. 40, where the necessary set of equations has been written down. However, the low frequency hysteresis loops of the assembly have not been constructed. The dynamics of magnetic nanoparticles in viscous liquid in alternating magnetic field was considered also in recent Ref. 41. Unfortunately, the authors<sup>41</sup> used the wrong expression for the regularly torque,  $N_m$  (see Eq. (2) below) in their equation for the rotational motion of the particle in liquid (Eq. (11) in Ref. 41). This makes their results doubtful.

In this paper, the problem is studied using the stochastic equations of motion<sup>33,34</sup> for the unit magnetization vector  $\alpha$  and the unit vector  $n$ , which determines the space orientation of a magnetic nanoparticle with uniaxial anisotropy. By solving these equations, one can describe in detail both the relaxation of the magnetic moment of a dilute assembly of superparamagnetic particles in a constant magnetic field and the behavior of the assembly in the low-frequency alternating magnetic field of finite amplitude. In this paper, we show that there are basically two regimes of the stationary magnetization oscillations, depending on the amplitude of the alternating magnetic field. They can be characterized as viscous and magnetic modes, respectively. The viscous regime occurs for low magnetic field amplitudes,  $H_0 \ll H_k$ , where  $H_k = 2K_1/M_s$  is the particle anisotropy field,  $K_1$  is the magnetic anisotropy constant and  $M_s$  is the saturation magnetization. In the viscous mode the unit vectors  $\alpha$  и  $n$  move in unison and out of phase with respect to the phase of the alternating magnetic field. In the opposite limit  $H_0 \geq H_k$ , the vector  $n$  oscillates only slightly, while the unit magnetization vector jumps between the states  $\alpha = \pm h_0$ , where  $h_0$  is the unit vector along the direction of the external magnetic field.

Interestingly, in both cases for stationary magnetization oscillations a partial or complete orientation of the assembly in viscous liquid occurs. The transition between the oscillation regimes occurs within the range  $0.5H_k \leq H_0 < H_k$ , depending on the magnetic field frequency and the liquid viscosity. In this paper, we describe in detail the behavior of the low-frequency hysteresis loops of the assembly as a function of the alternating magnetic field amplitude, frequency, and the liquid viscosity. The SAR of the assembly is calculated as a function of the frequency, viscosity, and other relevant parameters. Based on these calculations, we discuss the optimal conditions for an assembly of superparamagnetic nanoparticles in a liquid to absorb the energy of the alternating external magnetic field.

## II. BASIC EQUATIONS

Let us consider a behavior of a uniformly magnetized spherical nanoparticle with uniaxial magnetic anisotropy in a viscous liquid under the influence of a constant or alternating external magnetic field. Let  $n$  be the unit vector firmly attached to the particle. It shows the direction of the particle easy anisotropy axis. The kinematic equation of motion for this vector is given by

$$\frac{d\vec{n}}{dt} = [\vec{\omega}, \vec{n}], \quad (1)$$

where  $\omega$  is the angular velocity of the particle rotation as a whole. The rotational motion of the particle is described by a stochastic equation of motion<sup>33</sup>

$$I \frac{d\vec{\omega}}{dt} + \xi \vec{\omega} = \vec{N}_m + \vec{N}_{th}, \quad (2)$$

where  $I$  is the moment of inertia of a spherical particle,  $\xi = 6\eta V$  is the friction coefficient,  $\eta$  is the dynamic viscosity of the liquid, and  $V$  is the particle volume. The friction coefficient is determined by solving the problem<sup>42</sup> of rotation of a particle in a viscous liquid in the Stokes approximation for a small Reynolds number. In Eq. (2),  $N_m$  is the regularly torque associated with the particle magnetic moment and the  $N_{th}$  is the fluctuating torque that leads to a free Brownian rotation of the particle in a liquid in the absence of external magnetic field.

Dynamics of the unit magnetization vector  $\alpha$  of a single-domain nanoparticle is described by the stochastic Landau-Lifshitz equation<sup>10–12</sup>

$$\frac{\partial \vec{\alpha}}{\partial t} = -\gamma_1 [\vec{\alpha}, \vec{H}_{ef} + \vec{H}_{th}] - \kappa \gamma_1 [\vec{\alpha}, [\vec{\alpha}, \vec{H}_{ef} + \vec{H}_{th}]], \quad (3)$$

where  $\gamma_1 = |\gamma_0|/(1 + \kappa^2)$ ,  $\kappa$  is the damping constant and  $\gamma_0$  is the gyromagnetic ratio. In Eq. (3),  $H_{ef}$  is a vector of the effective magnetic field and  $H_{th}$  is a random magnetic field associated with the presence of thermal fluctuations in the system.

The total magnetic energy of the particle in an external uniform magnetic field  $H_0$  is given by

$$W = -K_1 V (\vec{\alpha} \vec{n})^2 - M_s V (\vec{\alpha} \vec{H}_0). \quad (4)$$

In the alternating magnetic field of a frequency  $f$  the vector  $H_0$  is replaced by  $H_0 \cos(\omega t)$ , where  $\omega = 2\pi f$  is the angular frequency. The effective magnetic field in Eq. (3) is the derivative of the total energy

$$\vec{H}_{ef} = -\frac{\partial W}{\partial \vec{\alpha}} = \vec{H}_0 + H_k (\vec{\alpha} \vec{n}) \vec{n}. \quad (5)$$

Similarly, the regularly torque in Eq. (2) can be calculated as

$$\vec{N}_m = \left[ \frac{\partial W}{\partial \vec{n}}, \vec{n} \right] = -2K_1 V (\vec{\alpha} \vec{n}) [\vec{\alpha}, \vec{n}]. \quad (6)$$

Note that Eq. (6) is a direct consequence of the general Lagrange principle.<sup>42</sup> It differs from the wrong expression,

$\vec{N}_m = [\vec{\mu}, \vec{H}_0] = M_s V [\vec{z}, \vec{H}_0]$ , used in Eq. (11) of Ref. 41 to describe the mechanical rotation of a magnetic nanoparticle in a viscous liquid.

In accordance with the fluctuation-dissipation theorem<sup>11</sup> the components of the fluctuating torque  $N_{th}$  have the following statistical properties<sup>33,43</sup> ( $i, j = x, y, z$ ):

$$\langle N_{th,i}(t) \rangle = 0; \quad \langle N_{th,i}(t) N_{th,j}(t_1) \rangle = 2k_B T \zeta \delta_{ij} \delta(t - t_1), \quad (7)$$

where  $k_B$  is the Boltzmann constant and  $T$  is the absolute temperature. For the components of the fluctuating magnetic field  $H_{th}$  similar relations<sup>10,11</sup> are supposed to be valid

$$\langle H_{th,i}(t) \rangle = 0; \quad \langle H_{th,i}(t) H_{th,j}(t_1) \rangle = \frac{2k_B T \kappa}{|\gamma_0| M_s V} \delta_{ij} \delta(t - t_1). \quad (8)$$

The set of Eqs. (1)–(8) can be simplified, if one takes into account<sup>31</sup> that because of a very small size of the magnetic nanoparticle it is possible to neglect in Eq. (2) the effective moment of inertia, assuming  $I \approx 0$ . Then, one obtains from Eqs. (1), (2), and (6) an equation of motion for the vector  $\mathbf{n}$  as follows:

$$\frac{\partial \vec{n}}{\partial t} = G(\vec{\alpha} \vec{n}) \left( \vec{\alpha} - (\vec{\alpha} \vec{n}) \vec{n} \right) - \frac{1}{\zeta} [\vec{n}, \vec{N}_{th}], \quad (9)$$

where  $G = 2K_1 V / \zeta = K_1 / 3\eta$ . It is interesting to note that the coefficient  $G$  does not depend on the particle radius. Equations (3) and (9), together with Eqs. (7) and (8) constitute a complete set of equations describing the behavior of a magnetic nanoparticle in a viscous liquid under the influence of the external ac or dc magnetic field. They have to be solved together using the corresponding numerical procedure (see Appendix).

In this paper, the illustrative calculations are performed for an assembly of uniaxial nanoparticles with magnetic parameters typical of the particles of iron oxides,  $K_1 = 10^5$  erg/cm<sup>3</sup>,  $M_s = 400$  emu/cm<sup>3</sup>. Therefore, the anisotropy field of the particle is given by  $H_k = 500$  Oe. The magnetic damping constant is assumed to be  $\kappa = 0.5$ . The viscosity of the liquid varies from the value typical for water,  $\eta = 0.01$  g/(cm s), when the coefficient  $G = 3.3 \times 10^6$  s<sup>-1</sup>, to a sufficiently large value  $\eta = 1.0$  g/(cm s). In the latter case, one has  $G = 3.3 \times 10^4$  s<sup>-1</sup>.

Let us assume the value  $C = 2 \cdot 10^{-6}$  erg/cm for the exchange constant of the magnetic material. Then, the characteristic single-domain radius of the nanoparticle can be estimated using Brown's<sup>44,45</sup> lower and upper estimates. As shown by Brown,<sup>44</sup> for the lower bound to the single-domain radius one can take  $a_c^{low} = x_1 R_0 / \sqrt{N}$ , where  $R_0 = \sqrt{C} / M_s$  is the exchange length,  $N = 4\pi/3$  is the demagnetizing factor of a sphere and  $x_1 = 2.0816$  is the minimal root of the spherical Bessel function derivative. As an upper bound for a soft magnetic nanoparticle ( $K_1 < M_s^2$ ) one can use the critical radius of stability<sup>45</sup> of a uniform magnetization,  $a_c^{up} = x_1 R_0 / \sqrt{N - 2K/M_s^2}$ . Then, for a particle with given magnetic parameters one finds  $R_0 = 35.4$  nm,  $a_c^{low} = 36$  nm,  $a_c^{up} = 43$  nm. Therefore, the single-domain diameter of the nanoparticles studied lies in the range  $72 \text{ nm} < D_c < 86 \text{ nm}$ . In this paper, the calculations are carried out for particles

with diameters  $D \leq 60$  nm. Therefore, it can be safely assumed that the magnetic behavior of a particle is mainly determined by a uniform rotation mode.<sup>46</sup>

### III. MAGNETO-DYNAMICS (MD) APPROXIMATION

It is instructive to consider first the dynamics of magnetic nanoparticles in a liquid neglecting the thermal fluctuations, i.e., dropping in Eqs. (3) and (9) the fluctuating terms  $N_{th}$  and  $H_{th}$ . This approximation<sup>31,32</sup> may be called the MD one. It is similar to the Stoner–Wohlfarth<sup>46</sup> approximation in the theory of a single-domain particle, when the influence of the thermal fluctuations on the particle behavior is completely neglected. We shall see below, in Sec. IV, that the MD approximation is very useful for a better understanding of the results of numerical simulation of the complete set of Eqs. (3) and (7)–(9), which take into account the effect of thermal fluctuations. In the MD approximation, the behavior of the particles in a liquid depends significantly on the amplitude of the external alternating magnetic field. Let us consider two characteristic cases.

#### A. Small magnetic field amplitude, $H_0 \ll H_k$

This limit may be called a viscous mode of magnetization oscillations, because in this case the power absorption is mainly due to viscous losses associated with the particle rotation in a liquid. Let us fix a relatively small amplitude of the alternating magnetic field,  $H_0 = 30$  Oe, as compared to the particle anisotropy field,  $H_k = 500$  Oe, and will gradually increase the frequency, assuming the liquid viscosity to be low,  $\eta = 0.01$  g/(cm s). In a stationary motion, which occurs after several periods of oscillation of the alternating magnetic field elapsed, the information about the initial positions of the vectors  $\alpha$  and  $\mathbf{n}$  is completely lost. As Figure 1(a) shows, at low frequency,  $f = 10$  kHz, in stationary motion the vectors  $\alpha$  and  $\mathbf{n}$  oscillate between the directions  $\pm \mathbf{h}_0$  and remain almost parallel to each other. Consequently, the magnetic moment of the assembly is changed due to the rotation of magnetic nanoparticles in a liquid as a whole. As seen in Fig. 1(a), the phase of the stationary oscillations of the vectors  $\alpha$  and  $\mathbf{n}$  is shifted by  $\pi/2$  with respect to that of the ac magnetic field.

As Fig. 1(b) shows, with increase in the frequency the amplitude of the oscillation of the vectors  $\alpha$  and  $\mathbf{n}$  along the magnetic field direction is greatly reduced. This means that these unit vectors rotate almost perpendicular to the vector  $\mathbf{h}_0$ . In this position, they oscillate in unison with relatively small amplitude. The phase of the oscillations is still shifted with respect to the phase of the alternating magnetic field. It is found that the amplitude of the oscillations increases as a function of  $H_0$ . On the contrary, the increase in viscosity (see Fig. 1(c)) leads to a decrease of the oscillation amplitude again. Also, a relative phase shift appears for  $\alpha$  and  $\mathbf{n}$  oscillations.

Nevertheless, for all cases considered the motion of the vectors  $\alpha$  and  $\mathbf{n}$  in the viscous mode is qualitatively the same. In fact, at a sufficiently high frequency,  $f \geq 100$  kHz, for every nanoparticle in stationary movement the vectors  $\alpha$  and  $\mathbf{n}$  oscillate being nearly perpendicular to the vector  $\mathbf{h}_0$ .



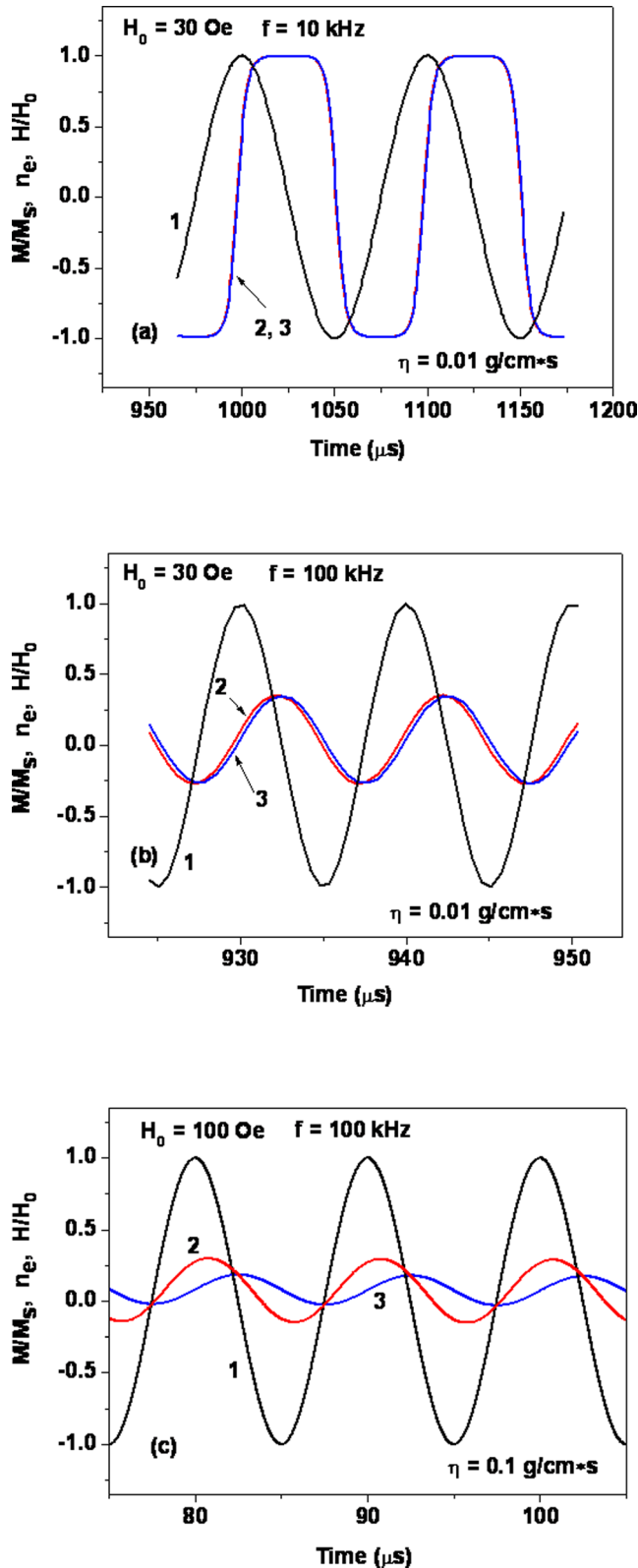


FIG. 1. The stationary MD oscillations of the components of the unit magnetization vector (2) and the particle director (3) along the magnetic field direction for various cases: (a)  $H_0 = 30$  Oe,  $f = 10$  kHz; (b)  $H_0 = 30$  Oe,  $f = 100$  kHz; (c)  $H_0 = 100$  Oe,  $f = 100$  kHz;  $\eta = 0.1$  g/(cm s). Curve (1) shows the oscillations of the reduced alternating magnetic field.

Thus, there is a partial orientation of a dilute assembly of nanoparticles in a liquid, as in the spherical coordinates  $(\theta, \varphi)$  the distribution of the directors of different nanoparticles is concentrated near the spherical angle  $\theta = \pi/2$ .

As Fig. 2 shows, in the stationary magnetization oscillations the area of MD hysteresis loop is finite. As we have seen above, in the viscous mode the vectors  $\alpha$  and  $n$  move in unison, so that the deviation of the magnetic vector from the easy anisotropy axis is small, as a rule. Nevertheless, there is a phase shift between the magnetic moment oscillations and the oscillations of the alternating magnetic field. Thus, there is a nonzero absorption of the energy of alternating external magnetic field. It is clear that in the viscous mode the power absorption is related mainly with the viscous friction during the particle rotation in a liquid.

It is well known<sup>5,9,39</sup> that the specific absorption rate is proportional to the area of the assembly hysteresis loop. As Fig. 2(a) shows, in the viscous mode the MD hysteresis loop area decreases rapidly with increasing frequency. Indeed, the magnetic field cannot rotate the particles to large angles due to their inertia associated with the viscous friction. Similarly, as shown in Fig. 2(b), in the viscous mode the hysteresis loop area decreases sharply with increasing of viscosity, as the amplitude of the unit magnetization vector oscillations along the magnetic field direction decreases.

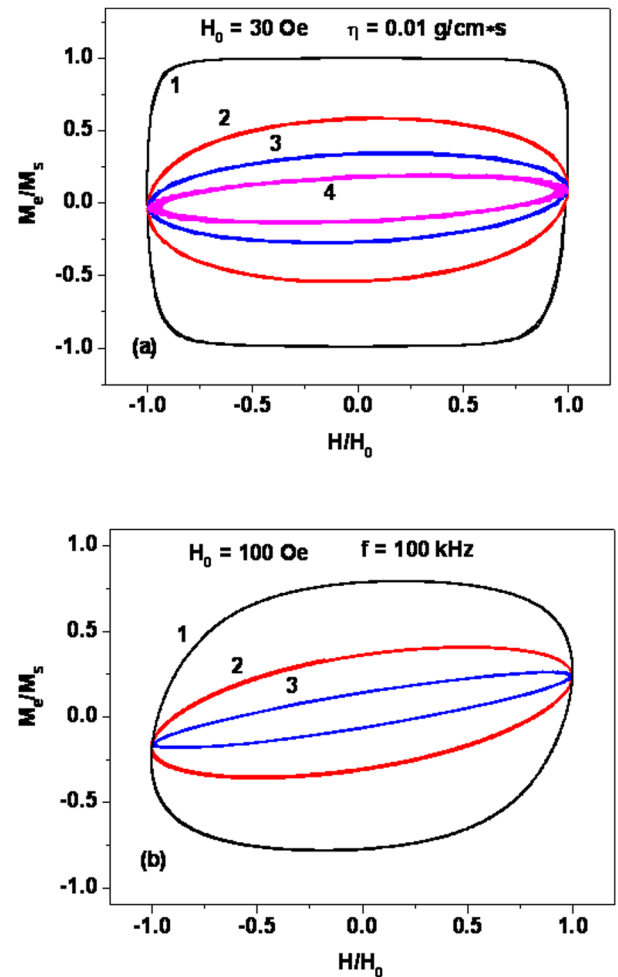


FIG. 2. (a) MD hysteresis loops of a particle in liquid in the viscous mode,  $H_0 < H_k$ , for various frequencies: (1)  $f = 10$  kHz, (2)  $f = 50$  kHz, (3)  $f = 100$  kHz, (4)  $f = 200$  kHz; (b) MD loops as a function of the liquid viscosity: (1)  $\eta = 0.01$  g/(cm s), (2)  $\eta = 0.03$  g/(cm s), (3)  $\eta = 0.1$  g/(cm s).

## B. Large magnetic field amplitude, $H_0 \geq H_k$

In this case, the mode of the stationary oscillations is simpler. As calculations show, for any initial direction of the vector  $\mathbf{n}$ , after a few oscillation periods this vector sets almost parallel to the field direction. This means that  $\mathbf{n} \approx \mathbf{h}_0$ , or  $\mathbf{n} \approx -\mathbf{h}_0$ , depending on the initial conditions. As Fig. 3(a) shows, the vector  $\mathbf{n}$  oscillates in this position with a very small amplitude, while the magnetic vector jumps between the states  $\alpha = \pm \mathbf{h}_0$ , moving from one magnetic potential well to another. The regime of magnetic oscillations observed in the limit  $H_0 \geq H_k$  may be called a magnetic mode, since in this case the behavior of the magnetic vectors is similar to that for an assembly of oriented nanoparticles immobilized in the solid matrix.

It is important to note that in the magnetic mode there is almost complete orientation of an assembly of magnetic nanoparticles in a liquid, because the directors of various nanoparticles point along the magnetic field direction. As a result, the shape of the MD hysteresis loop in the magnetic mode is close to rectangular. Clearly, in this case, the energy absorption is certainly determined by the magnetization

relaxation process, since the contribution to the energy absorption of the viscous friction is small.

In contrast to the viscous mode, the increase of the field frequency or the liquid viscosity does not change much the shape of the MD hysteresis loop in the magnetic mode. It is found that at  $H_0 = H_k$  the MD hysteresis loop shape is weakly dependent on frequency in the frequency range  $f = 100\text{--}800\text{ kHz}$ , and on the liquid viscosity in the range  $\eta = 0.01\text{--}0.1\text{ g/(cm s)}$ . The effect of viscosity becomes appreciable only at  $\eta = 1.0\text{ g/(cm s)}$ .

At low frequencies,  $f \sim 10\text{ kHz}$ , and viscosity  $\eta = 0.01$  the viscous mode exists for  $H_0 < 0.5H_k$ , and the magnetic mode is already realized at  $H_0 \geq 0.5H_k$ . However, in the MD approximation the critical field for transition to the magnetic mode increases gradually as a function of frequency. As Fig. 3(b) shows, at  $H_0 = 0.5H_k$  the MD hysteresis loop is still nearly rectangular at  $f = 100\text{ kHz}$ , but its area decreases gradually as the function of frequency. Actually, it is found that at  $f = 500\text{ kHz}$  the magnetic mode is realized at  $H_0 \geq 0.7H_k$  only.

For the most interesting viscous mode of the magnetization oscillations one can get an approximate analytical solution, which confirms the numerical results presented in Figs. 1 and 2. As shown below, for the viscous mode the intrinsic magnetic damping of the particle is negligible, so that the behavior of the vectors  $\alpha$  and  $\mathbf{n}$  is approximately described by a pair of equations that follow from Eqs. (3) and (9)

$$\frac{\partial \vec{\alpha}}{\partial t} = -\gamma[\vec{\alpha}, \vec{H}_0 \cos(\omega t) + H_k(\vec{\alpha}\vec{n})\vec{n}], \quad (10a)$$

$$\frac{\partial \vec{n}}{\partial t} = G(\vec{\alpha}\vec{n})\left(\vec{\alpha} - (\vec{\alpha}\vec{n})\vec{n}\right). \quad (10b)$$

As Fig. 1 shows, for the viscous mode,  $H_0 < H_k$ , the vectors  $\alpha$  and  $\mathbf{n}$  are always close, so that it is reasonable to put

$$\vec{n} = \vec{\alpha} + [\vec{\alpha}, \vec{\varepsilon}], \quad |\vec{\varepsilon}| \ll 1. \quad (11)$$

Eq. (10) can be rewritten as follows:

$$\frac{\partial \vec{\alpha}}{\partial t} = -\gamma[\vec{\alpha}, \vec{H}_0 \cos(\omega t) + H_k[\vec{\alpha}, \vec{\varepsilon}]], \quad (12a)$$

$$\frac{\partial}{\partial t}(\vec{\alpha} + [\vec{\alpha}, \vec{\varepsilon}]) = -G[\vec{\alpha}, \vec{\varepsilon}]. \quad (12b)$$

In the left-hand side of Eq. (12b), the correction term proportional to a small vector  $\varepsilon$  can be omitted. Then, substituting Eq. (12b) in Eq. (12a), one obtains an equation for the vector  $\alpha$

$$\frac{\partial \vec{\alpha}}{\partial t} = -\gamma[\vec{\alpha}, \vec{H}_0 \cos(\omega t)] + \frac{\gamma H_k}{G} \left[ \vec{\alpha}, \frac{\partial \vec{\alpha}}{\partial t} \right]. \quad (13a)$$

Having in hand the solution of Eq. (13a), one can obtain vector  $\mathbf{n}$  by means of the relation

$$\vec{n} = \vec{\alpha} - G \frac{\partial \vec{\alpha}}{\partial t}. \quad (13b)$$

Note that equation (13a) is the Landau-Lifshitz-Gilbert equation,<sup>10–12</sup> which describes a precession of the unit

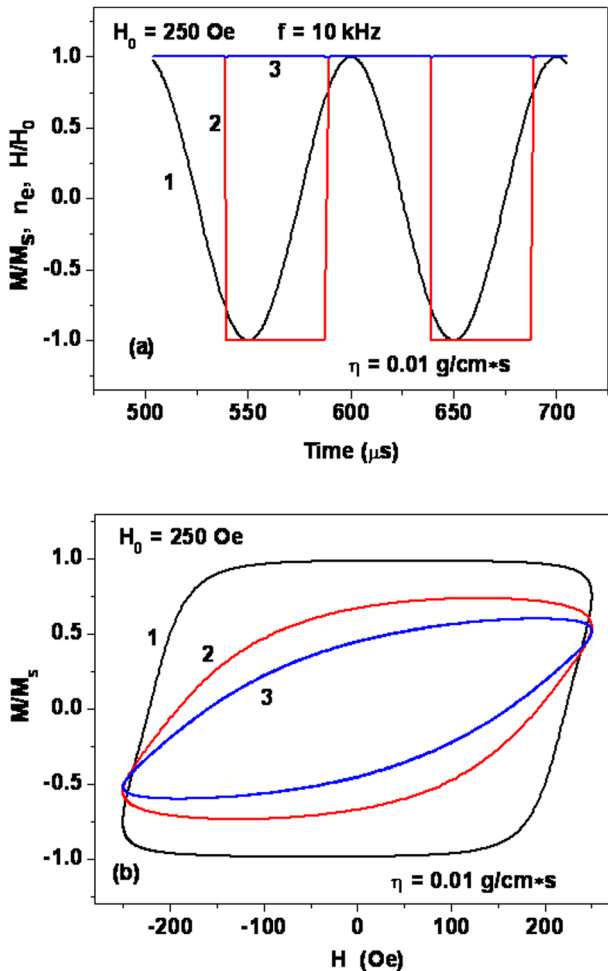


FIG. 3. (a) The stationary MD oscillations of the unit magnetization vector (2) and the particle director (3) at  $f = 10\text{ kHz}$  in the magnetic mode,  $H_0 = 0.5H_k$ , in comparison with the oscillations of the reduced magnetic field, curve 1; (b) MD hysteresis loops at  $H_0 = 0.5H_k$  for different frequencies: (1)  $f = 100\text{ kHz}$ , (2)  $f = 300\text{ kHz}$ , (3)  $f = 500\text{ kHz}$ .

magnetization vector  $\alpha$  in the magnetic field  $H_0$  in the presence of a large effective damping  $\mu = \gamma H_k / G = 6\gamma\eta / M_s \gg 1$ . Indeed, setting  $\gamma = 1.7 \times 10^7 \text{ Oe}^{-1}\text{s}^{-1}$ ,  $\eta = 0.01 \text{ g/(cm s)}$ , and  $M_s = 400 \text{ emu/cm}^3$  one obtains  $\mu = 2.55 \times 10^3$ . Evidently, the effective damping only increases as a function of the liquid viscosity.

Equation (13a) has an exact solution. In the spherical coordinates  $(\theta, \phi)$  with the polar axis along the vector  $h_0$ , the components of the unit magnetization vector are given by  $\alpha_x = \sin\theta\cos\phi$ ,  $\alpha_y = \sin\theta\sin\phi$ , and  $\alpha_z = \cos\theta$ . For the spherical angles, one obtains from Eq. (13a) the set of equations

$$\frac{d\theta}{dt} = -\mu\sin\theta\frac{d\phi}{dt}; \quad \frac{d\phi}{dt} = \frac{\gamma H_0 \cos(\omega t)}{1 + \mu^2}. \quad (14)$$

The integration of Eq. (14) gives

$$\phi(t) = \phi_0 + B\sin(\omega t), \quad \tan\frac{\theta(t)}{2} = C\exp(-\mu B\sin(\omega t));$$

$$B = \frac{\omega_H}{\omega(1 + \mu^2)}. \quad (15)$$

Here,  $\omega_H = \gamma H_0$ ;  $\phi_0$  and  $C$  are the constants of integration. It is convenient to set  $C = 1$ . Then, at  $t = \pi n / \omega$ ,  $n = 0, 1, \dots$ , when the external magnetic field is given by  $H_0(t) / H_0 = \pm h_0$ , the angle  $\theta(t) = \pi/2$ , i. e., the vector  $\alpha$  is perpendicular to  $h_0$ . According to Eq. (15), the angle  $\theta$  varies between the limits  $\theta_{\min} = 2\arctan(\exp(-\mu B))$ , and  $\theta_{\max} = 2\arctan(\exp(\mu B))$ . The amplitude of these oscillations is determined by the dimensionless parameter  $\mu B \approx \omega_H / \omega \mu$ . It is clear that with increasing  $\omega$  the parameter  $\mu B$  decreases and the oscillations of the angle  $\theta$  occur near the value  $\theta = \pi/2$ . Note that for a typical case  $H_0 = 100 \text{ Oe}$ ,  $f = 100 \text{ kHz}$ , and  $\eta = 0.01 \text{ g/(cm s)}$ , one obtains  $\mu B \approx 1$ . Thus, in this case the constant  $B \approx 1/\mu \ll 1$ , so that the vectors  $\alpha$  and  $n$  oscillate nearly in the same plane,  $\phi(t) \approx \phi_0$ .

#### IV. BEHAVIOR OF SUPERPARAMAGNETIC NANOPARTICLES

The MD approximation is useful for understanding the basic features of the dynamics of magnetic nanoparticles in a viscous liquid. However, the thermal fluctuations have a significant impact on the nanoparticle behavior. Nevertheless, in this section, we show that the MD hysteresis loops are often reproduced in the limit of large particle diameters when their magnetic moments are relatively stable with respect to thermal agitation. To analyze the behavior of superparamagnetic nanoparticles in an alternating external magnetic field, the complete set of the stochastic equations (3), (7)–(9) should be considered. The solution of the set is performed by using the well known algorithms [47–49] (see also Appendix).

To ensure the accuracy of the simulations performed, we use Mil'shtein scheme<sup>47,48</sup> and keep the physical time step lower than 1/50 of the characteristic particle precession time. For every particle diameter, a time-dependent particle magnetization  $M(t) = M_s \alpha(t)$  is calculated in a sufficiently large series of the numerical experiments,  $N_{\text{exp}} = 500\text{--}1000$ , for the same frequency and magnetic field amplitude.

Because various runs of the calculations are statistically independent, the component of the dilute assembly magnetization along the magnetic field direction is obtained<sup>12</sup> as an average value,  $\langle M_e(t) \rangle$ . Note, that the hysteresis loops shown below correspond to a stationary regime that is achieved after sufficient number of periods of the alternating magnetic field has been elapsed. All calculations are carried out at a room temperature,  $T = 300 \text{ K}$ , for particles with the same magnetic parameters as in Sec. III.

##### A. Viscous mode

Fig. 4(a) shows the evolution of the thermal hysteresis loop as a function of the particle diameter in a typical viscous mode,  $f = 100 \text{ kHz}$ ,  $H_0 = 100 \text{ Oe}$ . It is seen that with increasing particle diameter the thermal hysteresis loops approach ultimate MD loop, because the effect of the thermal fluctuations on the dynamics of the unit magnetization vector decreases. However, the MD loop is not reached even for a rather large single-domain nanoparticle with diameter

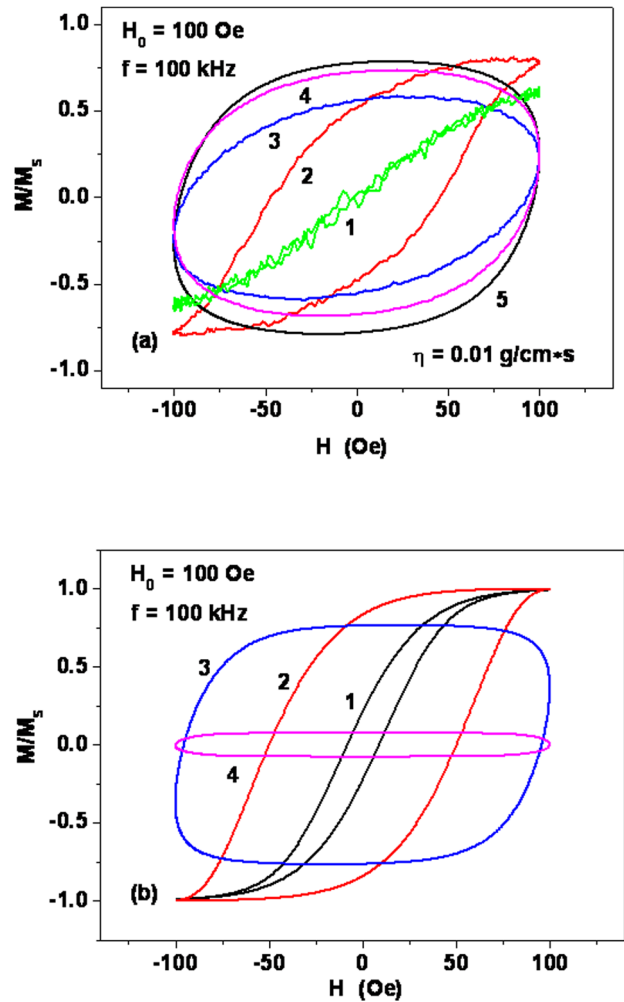


FIG. 4. (a) The thermal hysteresis loops of an assembly in liquid in the viscous mode as a function of the particle diameter: (1)  $D = 16 \text{ nm}$ , (2)  $D = 20 \text{ nm}$ , (3)  $D = 28 \text{ nm}$ , (4)  $D = 60 \text{ nm}$ , (5) ultimate MD loop; (b) The hysteresis loops of oriented assembly of immobilized nanoparticles with the same magnetic parameters as a function of the diameter: (1)  $D = 18 \text{ nm}$ , (2)  $D = 20 \text{ nm}$ , (3)  $D = 22 \text{ nm}$ , (4)  $D = 24 \text{ nm}$ .



$D = 60$  nm, because the thermal fluctuations of the director remain appreciable at room temperature,  $T = 300$  K. Indeed, the characteristic Brownian relaxation time<sup>27,28</sup>  $\tau_B = 3\eta V/k_B T$  has only power dependence on the particle diameter. It changes slowly in comparison to the Neel–Brown relaxation time that has an exponential dependence on this parameter,<sup>10,11</sup>  $\tau_N = \tau_0 \exp(K_1 V/k_B T)$ , where  $\tau_0$  is a pre-exponential constant.

One can see in Fig. 4(a) that in the viscous mode the hysteresis loop area increases monotonically with increase in the nanoparticle diameter. This behavior is completely different from that of an assembly of superparamagnetic nanoparticles immobilized in a solid matrix.<sup>5</sup> Indeed, as Fig. 4(b) shows, for an assembly of immobilized nanoparticles with the same magnetic parameters, the hysteresis loop area first increases and then decreases rapidly, because in the limit  $H_0 \ll H_k$  the external magnetic field is unable to remagnetize the nanoparticles of sufficiently large diameters. Thus, for an assembly of nanoparticles in a solid matrix there is a rather narrow range of diameters (in the given case  $D = 20$ – $22$  nm) where the area of the assembly hysteresis loop has a maximum. It can be shown that, similarly to the MD approximation (see Fig. 2) in the viscous mode the area of the thermal hysteresis loop decreases as a function of the frequency or liquid viscosity.

## B. Magnetic mode

Fig. 5(a) shows the thermal hysteresis loops of the assembly for a magnetic mode,  $H_0 = H_k$ , for different particle diameters. With increase in diameter the influence of thermal fluctuations of the magnetic vector decreases rapidly. As a result, the thermal hysteresis loops monotonically approach to the corresponding MD loop. However, the thermal hysteresis loops do not reach the ultimate MD one again, since the thermal fluctuations of the director are still significant at a room temperature. Due to thermal fluctuations of the director the earlier switching of the unit magnetization vector occurs. Thus, the coercive force of the assembly is reduced in comparison with the ultimate MD loop. Note that the thermal hysteresis loop shape is approximately rectangular for all particle diameters, because in the magnetic mode the nanoparticle assembly in the liquid is oriented along the magnetic field direction.

In Fig. 5(b), we compare the thermal hysteresis loops of an assembly in a liquid with that of oriented assembly of nanoparticles immobilized in a solid matrix. Note that the hysteresis loops for an assembly of nanoparticles in liquid have a lower coercive force. The difference of the loops of the two assemblies in Fig. 5(b) is associated with a slight deviation of the director  $\mathbf{n}$  of the particle in liquid at the moments when the external magnetic field is close to the particle coercive force. Due to this deviation, which is impossible for an immobilized nanoparticle, the effective energy barrier is reduced and the unit magnetization vector jumps to another well in the lower magnetic field, as compared to the case of immobilized particle. Although in the magnetic mode the difference of the hysteresis loops for the two assemblies is not as striking as for the viscous mode, yet the

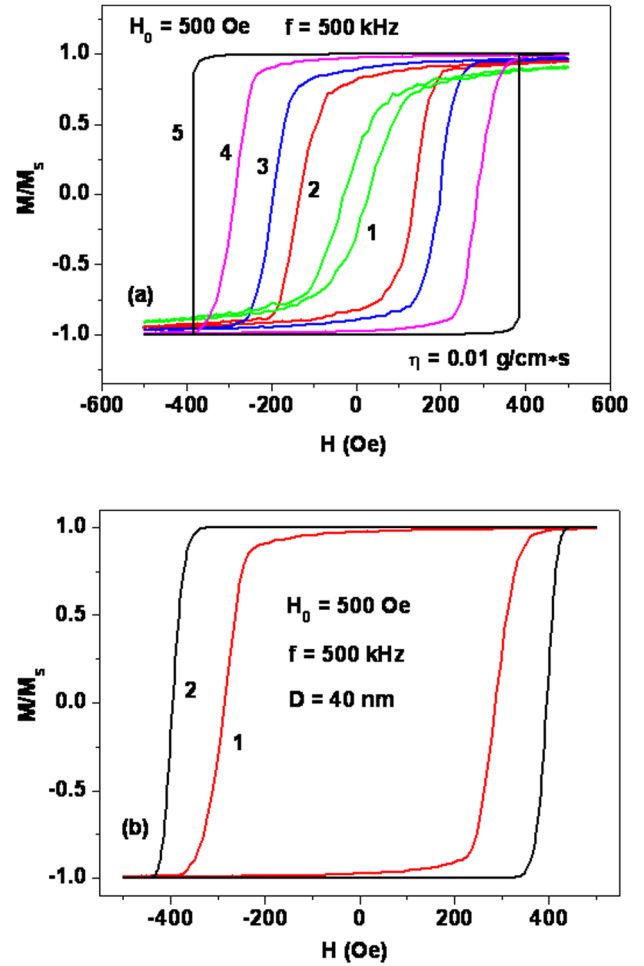


FIG. 5. (a) The thermal hysteresis loops of an assembly in liquid in the magnetic mode,  $H_0 = H_k$ ,  $f = 500$  kHz, as a function of the particle diameter: (1)  $D = 16$  nm, (2)  $D = 20$  nm, (3)  $D = 24$  nm, (4)  $D = 40$  nm, (5) ultimate MD loop; (b) The thermal hysteresis loop (1) of an assembly in liquid at  $\eta = 0.01$  g/(cm s) in comparison with that of oriented assembly (2) of the same nanoparticles immobilized in a solid matrix.

coercive force of the assembly in a liquid is smaller than that for the corresponding assembly of immobilized nanoparticles. As we have seen in Sec. III, the MD hysteresis loop in the magnetic regime,  $H_0 \geq H_k$ , are relatively weakly dependent on the field frequency and the liquid viscosity. In the magnetic mode, the thermal hysteresis loops show the same behavior too.

## C. The intermediate case, $H_0 \approx 0.5H_k$

It is interesting to consider this case separately, as in the MD approximation the transition between the magnetization oscillation modes occurs in the field interval  $0.5H_k \leq H_0 \leq H_k$ , depending on the field frequency and the liquid viscosity. As Fig. 6(a) shows, at a low frequency,  $f = 100$  kHz and  $H_0 = 300$  Oe the thermal hysteresis loops approach to the MD one with increase of the particle diameter. All these loops correspond to the magnetic mode. However, it is found that when frequency increases up to  $f = 500$  kHz, for the thermal hysteresis loops magnetic mode is realized at lower amplitudes as compared to the MD approximation. Indeed, as Fig. 6(b) shows, in this case the

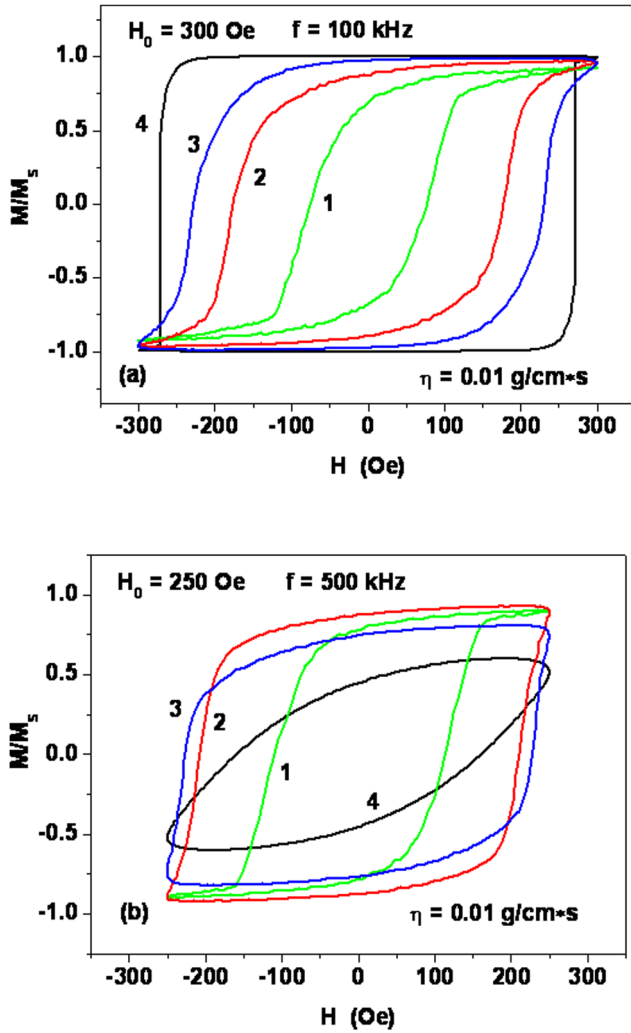


FIG. 6. (a) The thermal hysteresis loops of an assembly in liquid as a function of particle diameter at  $H_0 = 300$  Oe,  $f = 100$  kHz: (1)  $D = 20$  nm, (2)  $D = 28$  nm, (3)  $D = 48$  nm, (4) ultimate MD loop; (b) the same as in (a) but for  $H_0 = 250$  Oe,  $f = 500$  kHz: (1)  $D = 20$  nm, (2)  $D = 30$  nm, (3)  $D = 40$  nm, (4) MD loop.

thermal hysteresis loops are roughly rectangular and differ considerably from the corresponding MD loop. Therefore, at high enough frequency the presence of the thermal fluctuations lowers the characteristic field for the transition to the magnetic mode.

For practical applications in hyperthermia, it is important to provide a maximum squareness of the assembly hysteresis loop. Indeed, the SAR of the assembly is given by<sup>5,9</sup>  $\text{SAR} = A/\rho$ , where  $A$  is the area of the assembly hysteresis loop calculated in the variables  $(M, H)$ , and  $\rho$  is the density of the magnetic material. Therefore, the hysteresis loop having maximal squareness gives the maximum possible assembly SAR at a given frequency.<sup>5,9</sup> In Ref. 9 a dimensionless ratio  $A/A_{\max}$  is introduced where  $A_{\max} = 4M_s H_0$  is the ultimate value of the hysteresis loop area. Evidently, the assembly hysteresis loops with sufficiently large ratios  $A/A_{\max} \approx 1$  are optimal for hyperthermia. However, the loop area is also frequency dependent.

In the viscous regime at a low frequency for the nanoparticles of sufficiently large diameter the hysteresis loop

shape is close to rectangular. However, at a low frequency,  $f = 10$  kHz, the SAR of the assembly is relatively small. As we have seen in the Sec. IV A, in the viscous mode the increase in frequency leads to a significant decrease in the area of the thermal hysteresis loop. This implies that the viscous mode is hardly optimal for an assembly of magnetic nanoparticles in viscous liquid. Much higher SAR values for this assembly can be obtained in the magnetic mode, which also provides the high loop squareness due to the orientation of the assembly in the alternating magnetic field. However, the magnetic field of large amplitude,  $H_0 \sim H_k$ , is undesirable from both technical and medical points of view.<sup>1-4</sup> Actually, it is important to have appreciable SAR values at as small magnetic fields as possible, because the magnetic field strength decreases rapidly as a function of the distance from the magnetic field source. This fact can be essential for tumors located deeply in the living body. Therefore, the intermediate regime,  $H_0 \sim 0.5H_k$ , seems promising for magnetic hyperthermia, because in this case the hysteresis loop can be rectangular at sufficiently high frequencies.

It is important to note that for an assembly of nanoparticles in a liquid, contrary to an assembly of immobilized nanoparticles, the increase of the nanoparticle diameters only increases the hysteresis loop area. Accordingly, the large SAR values are expected for magnetic nanoparticle assemblies with sufficiently large particle diameters. They have to be close to the particle absolute single-domain size, when the magnetization reversal processes occurs by means of the uniform rotation mode.<sup>46</sup>

In Fig. 7, we show the calculated SAR values for a dilute assembly of nanoparticles in water,  $\eta = 0.01$  g/(cm s). The particle diameter is fixed at  $D = 40$  nm, the anisotropy field is equal to  $H_k = 500$  Oe, the density of particles is assumed to be  $\rho = 5$  g/cm<sup>3</sup>. In accordance with the above arguments, Fig. 7(a) shows that in the viscous mode,  $H_0 < 0.5H_k$ , the SAR of the assembly is relatively small and practically does not depend on the frequency. However, after the transition to the magnetic mode, even at  $H_0 = 0.5H_k$ , the SAR almost linearly increases with the frequency, since the hysteresis loop of the assembly in the magnetic mode is close to rectangular. Fig. 7(b) shows the dependence of the SAR on the magnetic field amplitude at a fixed frequency. Again one can see that at the frequency  $f = 500$  kHz a significant increase of the SAR occurs at  $H_0 = 0.5H_k$ , after the transition to the magnetic mode. One can see that for the given assembly the SAR increases more than twice in a relatively small field interval,  $200 \text{ Oe} < H_0 < 250 \text{ Oe}$ .

## V. DISCUSSION AND CONCLUSIONS

In this paper, the dynamics of a dilute assembly of superparamagnetic nanoparticles in a viscous liquid under the influence of external alternating magnetic field is studied theoretically. The results are obtained using numerical simulation of the stochastic equations of motion for the unit magnetization vector  $\alpha$  and the director  $\mathbf{n}$ . The latter describes the space orientation of the particle as a whole. It is shown that the dynamics of the particle in a liquid depends on the amplitude of the alternating magnetic field. In the viscous

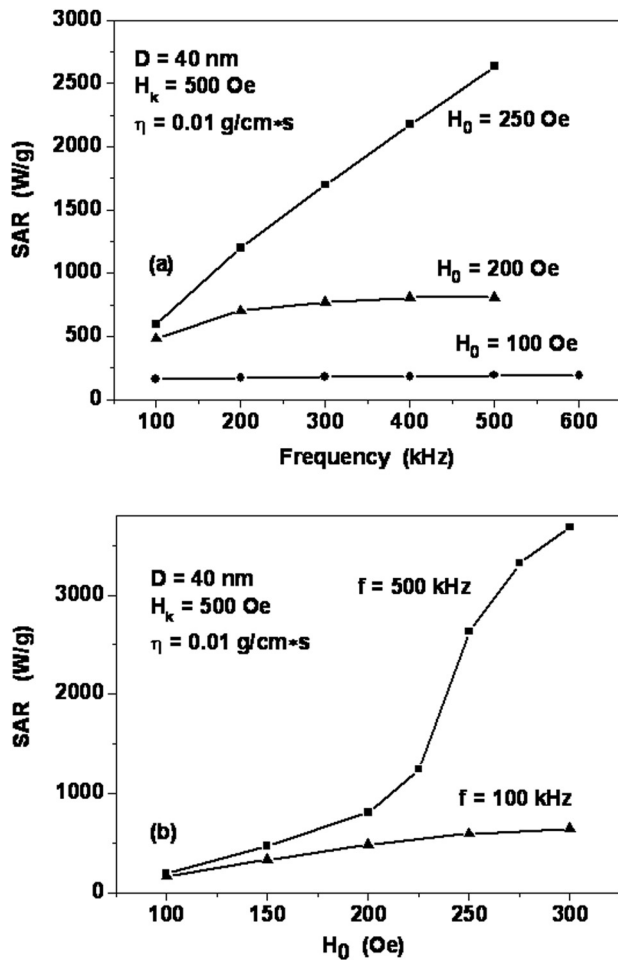


FIG. 7. SAR of a dilute assembly of uniaxial magnetic nanoparticles in a viscous liquid: (a) as a function of frequency at different  $H_0$  values and (b) as a function of field amplitude at various frequencies.

mode,  $H_0 \ll H_k$ , the particle generally rotates in a liquid as a whole, the vectors  $\alpha$  and  $n$  move in unison, and their oscillations are shifted in phase relative to that of the magnetic field oscillation. Therefore, the power absorption of the assembly is due mainly to the viscous losses in the liquid. The viscous regime is characterized by a sharp decrease in the hysteresis loop area with increasing both the frequency and viscosity of the liquid, because in both cases, the amplitude of the oscillations of the components of vectors  $\alpha$  and  $n$  parallel to the field direction, is dramatically reduced. In a stationary motion these vectors fluctuate being nearly perpendicular to the magnetic field direction. As a result, there is a partial orientation of an assembly of nanoparticles in the liquid at a sufficiently high frequency of the alternating magnetic field.

In the opposite regime,  $H_0 \geq H_k$ , in a stationary motion the director  $n$  oscillates slightly near the external magnetic field direction, whereas the unit magnetization vector  $\alpha$  sharply jumps between the states  $\pm h_0$ . Thus, a complete orientation of the assembly of nanoparticles in a liquid occurs in the alternating magnetic field of sufficient amplitude. The hysteresis loop shape of the assembly is nearly rectangular. It has relatively weak dependence on the magnetic field frequency and the liquid viscosity.

Thus, the magnetic dynamics of an assembly of magnetic nanoparticles in a liquid differs significantly from the behavior of the same assembly of nanoparticles immobilized in a solid matrix. In particular, for an assembly of nanoparticles in the liquid the hysteresis loop area increases monotonically with increasing particle diameter, since the magnetic moments of superparamagnetic nanoparticles with larger diameters are less susceptible to the thermal fluctuations. In contrast, for an assembly of nanoparticles immobilized in a solid matrix<sup>5</sup> there is a narrow range of diameters, where the hysteresis loop area has a maximum. Indeed, for  $H_0 < H_k$ , the magnetization reversal for the particles of sufficiently large diameter is not possible due to high value of the effective energy barriers.

For practical applications in magnetic nanoparticle hyperthermia, the assemblies with sufficiently large SAR are promising.<sup>2-4,9</sup> The SAR of the assembly in a liquid can be significantly increased by selecting a suitable mode of magnetization oscillations. It is shown in the present paper that for an assembly of nanoparticles in a liquid the intermediate excitation regime,  $H_0 \approx 0.5H_k$ , is preferable. Theoretical estimate gives for this case quite large SAR values, of the order of 1 kW/g, for an assembly with magnetic parameters typical for iron oxides, and for moderate values of  $H_0 = 200$ –300 Oe and  $f = 300$ –500 kHz.

The present study shows that the usual analysis of the experimental data<sup>3,16,17,19,23,24</sup> on the power absorption in a liquid made in a linear approximation,<sup>39</sup> and using the assumption of the effective relaxation time<sup>27,39</sup> is hardly adequate. Indeed, the introduction of the effective relaxation time is a formal receipt that does not take into account the complex dynamics of magnetic nanoparticles in a viscous liquid in an alternating external magnetic field of finite amplitude.

In fact, the orientation of an assembly of magnetic nanoparticles in a liquid in a strong alternating magnetic field has been experimentally observed in Refs. 22, 25, and 26. In particular, it has been found<sup>22</sup> that in sufficiently strong magnetic field there is even a spatial redistribution of the nanoparticles, so that they are self-organized into levitating needles elongated along the magnetic field direction. The authors of Refs. 25 and 26 claim that the approximate analytical expressions for the assembly hysteresis loop area and for the SAR (Ref. 9) are in qualitative agreement with their experimental measurements. Meanwhile, the analytical estimates<sup>9</sup> are derived under the implicit assumption that there is no rotation of the magnetic nanoparticles as a whole. On the other hand, the experimental results<sup>22,25,26</sup> were obtained for the assembly of nanoparticles dispersed in the liquid. Evidently, a significant difference in the behavior of the assemblies of nanoparticles dispersed in a liquid and immobilized in a solid matrix stated in the present paper has to be taken into account for a convincing interpretation of the experimental data. For a dense assembly of magnetic nanoparticles, it is necessary to take into account also the effect of strong magnetic dipole interactions between the magnetic nanoparticles. It has been shown experimentally<sup>50</sup> that the average demagnetizing field, which is determined by the demagnetizing factor of the whole nanoparticle assembly, has a very significant effect on the measured SAR value.

In conclusion, we would like to note that all calculations in this work are carried out under the assumption that the magnetic particle diameter is equal to its full diameter in the liquid. The rotational particle diameter in liquid is greater if there is a non-magnetic layer at the particle surface. However, the existence of a thin non-magnetic layer only leads to a small change in the regular and random torques in Eqs. (6) and (7). This effect can hardly significantly alter the results obtained in this paper.

## ACKNOWLEDGMENTS

Partial financial support from the Russian Foundation for Basic Research (Grant №10-02-01394-a) is gratefully acknowledged.

## APPENDIX: SOLUTION OF THE STOCHASTIC EQUATIONS

The procedure for solving the set of the stochastic equations (3), (7)–(9) is as follows. First, we introduce a dimensionless time  $t^* = t\gamma_1 H_t$  in Eqs. (3) and (9) using a characteristic magnetic field

$$H_t = \sqrt{H_0^2 + H_k^2}. \quad (\text{A1})$$

The reason for this is a high precession frequency of the unit magnetization vector. This vector is always moving much faster relative to the motion of the director  $\mathbf{n}$ . Next, we introduce the dimensionless fields in Eq. (3) setting  $h_{ef,i} = H_{ef,i}/H_t$ , and  $h_{th,i} = H_{th,i}/H_t$ , ( $i = x, y, z$ )

$$\frac{\partial \vec{\alpha}}{\partial t^*} = -[\vec{\alpha}, \vec{h}_{ef} + \vec{h}_{th}] - \kappa[\vec{\alpha}, [\vec{\alpha}, \vec{h}_{ef} + \vec{h}_{th}]]. \quad (\text{A2})$$

For the average components of the reduced random magnetic field, one obtains from Eq. (8) the relations

$$\begin{aligned} \langle h_{th,i}(t) \rangle &= 0; \quad \langle h_{th,i}(t^*) h_{th,j}(t_1^*) \rangle = \frac{\lambda \gamma_1}{H_t} \delta_{ij} \delta(t^* - t_1^*); \\ \lambda &= \frac{2k_B T \kappa}{|\gamma_0| M_s V}. \end{aligned} \quad (\text{A3})$$

In the integration of the stochastic Eq. (A2) by the known algorithm,<sup>47,48</sup> it is necessary to use Gaussian random numbers

$$\Delta W_{m,i} = \int_{t^*}^{t^*+dt^*} dt' h_{th,i}(t').$$

The statistical properties of these numbers follow from Eq. (A3)

$$\langle \Delta W_{m,i} \rangle = 0; \quad \langle \Delta W_{m,i} \Delta W_{m,j} \rangle = \frac{\lambda \gamma_1}{H_t} dt^* \delta_{ij} = \sigma_m^2 \delta_{ij},$$

where the corresponding dispersion is given by

$$\sigma_m = \sqrt{\frac{\lambda \gamma_1}{H_t} dt^*} = \left( \frac{2\kappa}{1 + \kappa^2} \frac{k_B T}{M_s H_t V} dt^* \right)^{1/2}.$$

Similarly, the dimensionless equation for the director is given by

$$\frac{\partial \vec{n}}{\partial t^*} = \frac{2K_1 V}{\xi \gamma_1 H_t} (\vec{\alpha} \vec{n}) (\vec{\alpha} - (\vec{\alpha} \vec{n}) \vec{n}) - \frac{1}{\varepsilon_0} [\vec{n}, \vec{N}_{th}], \quad (\text{A4})$$

where  $\varepsilon_0 = \xi \gamma_1 H_t$  is the characteristic energy. It is convenient to introduce dimensionless components of the random torque, setting  $\tilde{N}_{th,i} = N_{th,i}/\varepsilon_0$ . They have the following statistical properties

$$\langle \tilde{N}_{th,i} \rangle = 0; \quad \langle \tilde{N}_{th,i}(t^*) \tilde{N}_{th,j}(t_1^*) \rangle = \frac{2k_B T}{\varepsilon_0} \delta_{ij} \delta(t^* - t_1^*). \quad (\text{A5})$$

In the integration of the stochastic Eq. (A4), another Gaussian random numbers have to be used

$$\Delta W_{n,i} = \int_{t^*}^{t^*+dt^*} dt' \tilde{N}_{th,i}(t').$$

Their statistical properties follow from Eq. (A5)

$$\langle \Delta W_{n,i} \rangle = 0; \quad \langle \Delta W_{n,i} \Delta W_{n,j} \rangle = \frac{2k_B T}{\varepsilon_0} dt^* \delta_{ij} = \sigma_n^2 \delta_{ij}.$$

Here the corresponding dispersion is given by

$$\sigma_n = \left( \frac{2k_B T}{\varepsilon_0} dt^* \right)^{1/2}.$$

To integrate the stochastic Eqs. (A2) and (A4), a small increment of the dimensionless time,  $dt^* = 10^{-2} - 10^{-3}$ , has been used<sup>12</sup> in order to keep the physical time step sufficiently small in comparison with the characteristic particle precession time.

<sup>1</sup>Q. A. Pankhurst, N. K. T. Thanh, S. K. Jones, and J. Dobson, *J. Phys. D: Appl. Phys.* **42**, 224001 (2009).

<sup>2</sup>S. Laurent, S. Dutz, U. O. Häfeli, and M. Mahmoudi, *Adv. Colloid Interface Sci.* **166**, 8 (2011).

<sup>3</sup>R. Hergt, S. Dutz, R. Müller, and M. Zeisberger, *J. Phys.: Condens. Matter* **18**, S2919 (2006).

<sup>4</sup>R. Hergt, S. Dutz, and M. Röder, *J. Phys.: Condens. Matter* **20**, 385214 (2008).

<sup>5</sup>N. A. Usov, *J. Appl. Phys.* **107**, 123909 (2010).

<sup>6</sup>P.-M. Déjardin, Yu. P. Kalmykov, B. E. Kashevsky, H. El Mrabti, I. S. Poperechny, Yu. L. Raikher, and S. V. Titov, *J. Appl. Phys.* **107**, 073914 (2010).

<sup>7</sup>I. S. Poperechny, Yu. L. Raikher, and V. I. Stepanov, *Phys. Rev. B* **82**, 174423 (2010).

<sup>8</sup>E. Mrabti, S. V. Titov, P.-M. Déjardin, and Y. P. Kalmykov, *J. Appl. Phys.* **110**, 023901 (2011).

<sup>9</sup>J. Carrey, B. Mehdaoui, and M. Respaud, *J. Appl. Phys.* **109**, 083921 (2011).

<sup>10</sup>W. F. Brown, Jr., *Phys. Rev.* **130**, 1677 (1963).

<sup>11</sup>W. T. Coffey, Yu. P. Kalmykov, and J. T. Waldron, *The Langevin Equation*, 2nd ed. (World Scientific, Singapore, 2004).

<sup>12</sup>N. A. Usov and Yu. B. Grebenshchikov, "Micromagnetics of Small Ferromagnetic Particles," in *Magnetic Nanoparticles*, edited by S. P. Gubin (Wiley-VCH, 2009), Chap. 8.



- <sup>13</sup>R. Hergt, R. Hiergeist, I. Hilger, W. A. Kaiser, Y. Lapatnikov, S. Margel, and U. Richter, *J. Magn. Magn. Mater.* **270**, 345 (2004).
- <sup>14</sup>R. Hergt, R. Hiergeist, M. Zeisberger, D. Schüller, U. Heyen, I. Hilger, and W. A. Kaiser, *J. Magn. Magn. Mater.* **293**, 80 (2005).
- <sup>15</sup>S. Dutz, R. Hergt, J. Murbec, R. Muller, M. Zeisberger, W. Andra, J. Topfer, M. E. Bellemann *J. Magn. Magn. Mater.* **308**, 305 (2007).
- <sup>16</sup>J. P. Fortin, F. Gazeau, and C. Wilhelm, *Eur. Biophys. J.* **37**, 223 (2008).
- <sup>17</sup>M. Levy, C. Wilhelm, J.-M. Siaugue, O. Horner, J.-C. Bacri, and F. Gazeau, *J. Phys.: Condens. Matter* **20**, 204133 (2008).
- <sup>18</sup>M. Gonzales-Weimuller, M. Zeisberger, and K. M. Krishnan, *J. Magn. Magn. Mater.* **321**, 1947 (2009).
- <sup>19</sup>M. Suto, Y. Hirota, H. Mamiya, A. Fujita, R. Kasuya, K. Tohji, and B. Jeyadevan, *J. Magn. Magn. Mater.* **321**, 1493 (2009).
- <sup>20</sup>S. Dutz, J. H. Clement, D. Eberbeck, T. Gelbrich, R. Hergt, R. Muller, J. Wotschadlo, and M. Zeisberger, *J. Magn. Magn. Mater.* **321**, 1501 (2009).
- <sup>21</sup>B. Mehdaoui, A. Meffre, L.-M. Lacroix, J. Carrey, S. Lachaize, M. Respaud, M. Gougeon, and B. Chaudret, *J. Appl. Phys.* **107**, 09A324 (2010).
- <sup>22</sup>B. Mehdaoui, A. Meffre, L.-M. Lacroix, J. Carrey, S. Lachaize, M. Gougeon, M. Respaud, and B. Chaudret, *J. Magn. Magn. Mater.* **322**, L49 (2010).
- <sup>23</sup>A. P. Khandhar, R. M. Ferguson, and K. M. Krishan, *J. Appl. Phys.* **109**, 07B310 (2011).
- <sup>24</sup>C. H. Li, P. Hodgins, and G. P. Peterson, *J. Appl. Phys.* **110**, 054303 (2011).
- <sup>25</sup>B. Mehdaoui, A. Meffre, J. Carrey, S. Lachaize, L.-M. Lacroix, M. Gougeon, B. Chaudret, and M. Respaud, *Adv. Funct. Mater.* **21**, 4573 (2011).
- <sup>26</sup>B. Mehdaoui, J. Carrey, M. Stadler, A. Cornejo, C. Nayral, F. Delpech, B. Chaudret, and M. Respaud, *Appl. Phys. Lett.* **100**, 052403 (2012).
- <sup>27</sup>M. I. Shliomis, *Sov. Phys. Usp.* **17**, 153 (1974).
- <sup>28</sup>R. E. Rosensweig, *Ferrohydrodynamics* (Cambridge University Press, Cambridge, England, 1985).
- <sup>29</sup>K. Morozov, M. Shliomis, and M. Zahn, *Phys. Rev. E* **73**, 066312 (2006).
- <sup>30</sup>D. V. Berkov, L. Yu. Iskakova, and A. Yu. Zubarev, *Phys. Rev. E* **79**, 021407 (2009).
- <sup>31</sup>J. J. Newman and R. B. Yarbrough, *J. Appl. Phys.* **39**, 5566 (1968).
- <sup>32</sup>J. J. Newman and R. B. Yarbrough, *IEEE Trans. Magn.* **5**, 320 (1969).
- <sup>33</sup>W. T. Coffey and Yu. P. Kalmykov, *J. Magn. Magn. Mater.* **164**, 133 (1996).
- <sup>34</sup>D. V. Berkov, N. L. Gorn, R. Schmitz, and D. Stock, *J. Phys.: Condens. Matter* **18**, S2595 (2006).
- <sup>35</sup>P. C. Fannin, T. Relihan, and S. W. Charles, *Phys. Rev. B* **55**, 14423 (1997).
- <sup>36</sup>Yu. L. Raikher and V. V. Rusakov, *J. Magn. Magn. Mater.* **258–259**, 459 (2003).
- <sup>37</sup>P. C. Fannin, C. N. Marin, and C. Couper, *J. Magn. Magn. Mater.* **322**, 1682 (2010).
- <sup>38</sup>A. M. Rauwerdink and J. B. Weaver, *J. Magn. Magn. Mater.* **322**, 609 (2010).
- <sup>39</sup>R. E. Rosensweig, *J. Magn. Magn. Mater.* **252**, 370 (2002).
- <sup>40</sup>H. Xi, K.-Z. Gao, Y. Shi, and S. Xue, *J. Phys. D: Appl. Phys.* **39**, 4746 (2006).
- <sup>41</sup>H. Mamiya and B. Jeyadevan, *Sci. Rep.* **1**, 157 (2011).
- <sup>42</sup>L. D. Landau and E. M. Lifshitz, *Fluid Mechanics*, 2nd ed. (Pergamon, 1987).
- <sup>43</sup>K. A. Valiev and E. N. Ivanov, *Sov. Phys. Usp.* **16**, 1 (1973).
- <sup>44</sup>W. F. Brown, Jr., *Ann. N.Y. Acad. Sci.* **147**, 461 (1969).
- <sup>45</sup>W. F. Brown, Jr., *Micromagnetics* (Interscience, New York, 1993).
- <sup>46</sup>E. C. Stoner and E. P. Wohlfarth, *Phil. Trans. R. Soc. London, Ser. A* **240**, 599 (1948).
- <sup>47</sup>J. L. Garcia-Palacios and F. J. Lazaro, *Phys. Rev. B* **58**, 14937 (1998).
- <sup>48</sup>W. Scholz, T. Schrefl, and J. Fidler, *J. Magn. Magn. Mater.* **233**, 296 (2001).
- <sup>49</sup>D. V. Berkov, *IEEE Trans. Magn.* **38**, 2489 (2002).
- <sup>50</sup>S. A. Gudoshnikov, B. Ya. Liubimov, and N. A. Usov, *AIP Adv.* **2**, 012143 (2012).